Understanding and Exploiting Window Effects for Adsorption and Separations of Hydrocarbons

Luna-Triguero, A.; Vicent-Luna, J.M.; Dubbeldam, D.; Gómez-Álvarez, P.; Calero, S.

DOI
10.1021/acs.jpcc.5b05597

Publication date
2015

Document Version
Final published version

Published in
The Journal of Physical Chemistry. C

THE JOURNAL OF PHYSICAL CHEMISTRY C

Article

pubs.acs.org/JPCC

Understanding and Exploiting Window Effects for Adsorption and Separations of Hydrocarbons

A. Luna-Triguero,[†] J. M. Vicent-Luna,[†] D. Dubbeldam,[‡] P. Gómez-Álvarez,*[,†] and S. Calero*[,†]

[†]Department of Physical, Chemical and Natural Systems, Universidad Pablo de Olavide, ES-41013, Seville, Spain

[‡]Van't Hoff Institute for Molecular Sciences, University of Amsterdam, Science Park 904, 1098 XH Amsterdam, The Netherlands

Supporting Information

ABSTRACT: The suitability of zeolites for a certain application strongly depends on their structural features. Among the types of shape selectivity, there is the still quite unexplored "cage or window effect" consisting of an unusual nonmonotonic increase of the Henry coefficient with chain length in cagelike zeolites when the guest hydrocarbon becomes too long to fit comfortably inside the wider part of the cages. This phenomenon has been addressed for alkanes in various zeolites, but a study dealing with alkenes is lacking. Because of both scientific interest and the impact on the petrochemical industry, we aimed at assessing window effects for a variety of alkenes regarding the position and number of the double bond. We used advanced molecular simulation techniques and considered the rigid all-silica channel-like OFF and cagelike ERI, CHA, and ITQ-29 zeolites. Our study reveals results similar to those of alkanes when the double bond is located at the chain extremes. Conversely, less molecular flexibility induced by intermediate positions of the double bond or the presence of more than one bond lead to a weakness of the window effect, except for the ITQ-29 because of its considerably larger cage. These findings result in significant values of this type of selectivity for separations of saturated and unsaturated hydrocarbons with chain lengths commensurate with the zeolite cages.

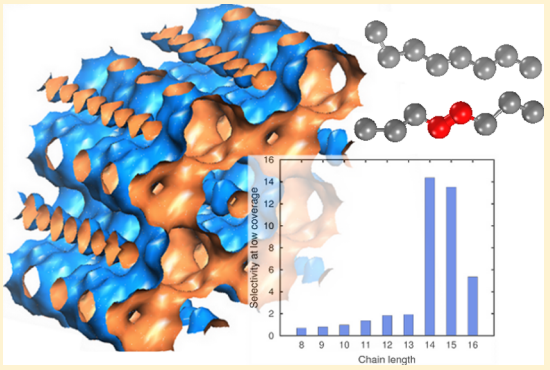

1. INTRODUCTION

Zeolites are nanoporous crystalline structures based essentially on tetrahedral coordinated T atoms, where T is usually silica or aluminum, linked together by oxygen atoms to shape a three-dimensional system of cavities of molecular dimensions. Different types of zeolites result from differences in the way the T atoms may join in the space. These materials are widely used as molecular sieves, cation exchangers, or catalysts in petrochemical applications. It is well-known that the performance of zeolites for a given task strongly depends on the structural features. While their active sites are related with catalytic activity of zeolites, the diameter, interconnectivity, and dimensionality of the pore system give rise to the molecular sieving action. This ability to discriminate among reactants, products, or reaction intermediates according to shape and size of pores is called shape selectivity, and it is of great importance and widely exploited in catalysis. Three main types of shape selectivity have been described, namely reactant shape selectivity (RSS),[1] product shape selectivity (PSS),[1] and restricted transition-state selectivity (TSS).[2] They are related with the effect of zeolite topology on the barriers to adsorption, desorption, and reaction, respectively. Other types are the subject of debate, such as the so-called "cage" or "window" effect.[3−7] The origin of the window effect is a relatively unfavorable adsorption for the chain lengths close to the cage size combined with a low orientational freedom as the chains are stretched across a cage tethered at opposite windows. For instance, the cavity of erionite has dimensions similar to the length of *n*-octane, which is responsible for the "window" effect. A deep molecular-level characterization of this phenomenon within the nanopores is essential to understand many processes of relevance, from a scientific point of view to industrial applications. In this regard, molecular simulation is a powerful tool that allows detailed exploration of the molecular arrangements of the confined fluid. Conventional molecular simulations are generally limited to relatively fast diffusing molecules or small rigid molecules, and only Dubbeldam et al.[8−11] addressed this subject for alkanes in various zeolites by using advanced molecular simulation techniques.[12−14] Overall, longer *n*-alkanes have more attractive adsorbent−adsorbate interactions and thus a lower adsorption enthalpy. Likewise, they have fewer conformations in the adsorbed phase as compared to the gas phase and thus lower adsorption entropy. The decrease in enthalpy offsets the decrease in entropy, so that the Gibbs free energy of adsorption decreases (and the Henry coefficient increases) with the lengthening of the *n*-alkane. However, their simulations indicated that the compensation theory applies for channel-type zeolites as OFF-type, which

Received: June 11, 2015
Revised: July 29, 2015
Published: July 30, 2015

DOI: 10.1021/acs.jpcc.5b05597
J. Phys. Chem. C 2015, 119, 19236−19243

exhibit the described usual monotonic increase of the Henry coefficient with the chain length. However, for cage-type zeolites with small windows, the described behavior occurs only for effective chain lengths much smaller than the cage size. From a certain alkane chain length of comparable size to the zeolite cage, their results revealed a distinct decrease in the Henry adsorption constants. The linear relationship breaks down. Instead of attractive adsorbate−adsorbent interactions, these windows exert repulsive adsorbate−adsorbent interactions that increase the adsorption enthalpy of any *n*-alkane partially adsorbed inside such a window. Accordingly, the usual compensation between adsorption enthalpy and adsorption entropy ceases as soon as *n*-alkanes become too long to fit comfortably inside the wider part of these pores (cages). For these *n*-alkanes, the loss of entropy with increasing length dominates their adsorption properties. Dubbeldam et al.[8−11] corroborated the existence of the window effect for ERI-type zeolite as well as for CHA and LTA sieves. The CHA-type cages are slightly shorter than the elongated ERI-type cages, and both cage types are significantly smaller than the spherical LTA-type cages. Therefore, the heats of adsorption in this zeolite were found also to be nonmonotonic but only for large alkanes, particularly those longer than 21 carbon atoms.

Despite the efforts on paraffins,[8−11,15] to our knowledge a study of this phenomenon dealing with olefins is lacking. However, this is crucial because separation of mixtures of alkane and alkene molecules is of great interest in the petrochemical industry. Besides, adsorption-based separations[16] of hydrocarbons are low-cost alternatives to other separation technologies, such us cryogenic distillation. Thus, in this work we evaluate the window effects for a variety of alkenes in regard to the position and number of double bonds. Specifically, we conducted configurational-bias Monte Carlo (CBMC) simulations to compute heats of adsorption and Henry coefficients and analyzed these magnitudes as a function of the carbon chain length. With the aim of comparing with alkanes, we also used the rigid all-silica OFF-, ERI-, CHA-, and LTA-type zeolites. From the Henry coefficients, we calculate the selectivity at dilute regime to assess the effectiveness of olefin−paraffin as well as olefin−olefin separations.

2. METHODS

The zeolite lattices (illustrated in Figure 1) were modeled as rigid crystals with the framework atoms placed at the crystallographic positions. Detailed structural description of these zeolites can be found elsewhere. We used the united-atom model reported by Liu et al.[17] for describing the alkenes. The CH_3 (sp3), CH_2 (sp3 and sp2), and CH (sp2) groups are thus considered as single interaction centers with their own effective potentials. The bonded interactions include bond-stretching, bond-bending, and torsion potentials. The beads in the chain are connected by harmonic bonding potentials. The bond bending between three neighboring beads is modeled by a harmonic cosine bending potential, and changes in the torsional angle are controlled by TraPPE cosine series potential. The beads in a chain separated by more than three bonds interact with each other through a Lennard-Jones potential. Nonbonded interactions consisted of dispersive Lennard-Jones interactions between guest molecules and also with the oxygen framework atoms. The interactions with the silica atoms are implicitly taken into account in this effective potential. The potential is cut and shifted with the cutoff distance set to 12 Å with periodic boundary conditions[18] exerted in the three

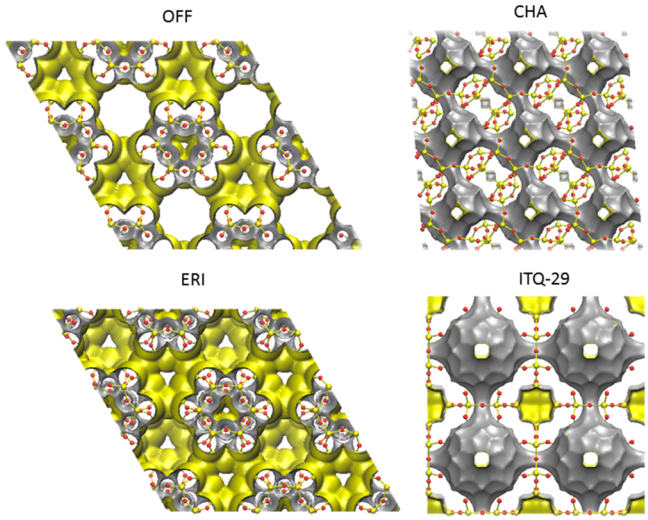

Figure 1. Atomic structure and solvent surface of the targeted zeolites.

dimensions. In all-silica structures, the electric field does not vary much across the channels and cages, and Coulomb contributions to the energy of the alkenes can be neglected. These force fields were proven to be suitable for accurately reproducing the adsorption properties of short alkenes in all-silica zeolites. Torsion interactions when the double bond is not located in the first position of the chain was described with a potential recently developed in our group on the basis of quantum calculations.[19] To establish a comparison, simulations of alkanes were also carried out by using parameters reported in Dubbeldam et al.[14] All used intra- and intermolecular force field parameters are summarized in Table S1 of the Supporting Information.

Using the above-described models and force fields, CBMC simulations were conducted to efficiently characterize the low-coverage adsorption of saturated and unsaturated hydrocarbons in the targeted porous structures. In the CBMC scheme, molecules are grown atom by atom, biasing the growth process toward energetically favorable configurations and avoiding overlap with the zeolite. A comprehensive description can be found in previously reported works.[12−14] Simulations were performed using the RASPA code.[20,21] We used the *NVT* ensemble with the Widom particle-insertion method[22] to account for the heats of adsorption, Q_{st}, and Henry coefficients, K_H. Both magnitudes were calculated for a wide range of chain lengths and at 600 K because this is the temperature of interest in catalytic processes. All simulations consist of 50 000 equilibration cycles and 2 000 000 production cycles. Likewise, molecular dynamics (MD) simulations in the *NVT* ensemble were conducted to characterize molecular conformations within the pores along the time. We fixed the temperature using Nose−Hoover thermostat.[23,24] We used a time step of 0.5 fs and executed the production runs for 10 million steps (5 ns).

3. RESULTS AND DISCUSSION

Because the adsorptive phenomenon under study is closely related to the topology and pore dimensions of the zeolite frameworks, a number of host properties were computed using Zeo++.[25] This is a software package used for analysis of crystalline porous materials from a geometric viewpoint on the basis of the Voronoi decomposition. On the one hand, two quantities of particular interest characterizing the pores are the

DOI: 10.1021/acs.jpcc.5b05597
J. Phys. Chem. C 2015, 119, 19236−19243

pore limiting diameter (PLD) and the largest cavity diameter (LCD). The PLD, also known as the maximum free sphere diameter,[26] is defined as the largest diameter that a sphere can have within the framework so that it can move through the structure without overlapping one or more frameworks atoms. The LCD, also called maximum included sphere diameter,[26] is defined as the largest spherical particle that can be inserted at some point within the pores without overlapping with any framework atoms. On the other hand, two important geometrical parameters characterizing the accessible space are surface area and pore volume. The accessible surface area (ASA), originally defined by Lee and Richards,[27] represents the surface traced by the center of a spherical probe as it is rolled along the atomic surface. The accessible volume (AV) can be analogously defined as the volume reachable by the center of the probe. Unlike pore sizes, these magnitudes are thus a function of the size of the guest molecules. Table 1 collects

Table 1. Characteristic Diameters and Accessible Space (Probe Radius = 1.3 Å) of the Zeolites Obtained Using Zeo++ Code[25]

	pore size			
zeolites	PLD [Å]	LCD [Å]	ASA [$m^2 \cdot g^{-1}$]	AV [$cm^3 \cdot g^{-1}$]
OFF	6.27	7.04	1056	0.0792
CHA	3.43	7.00	1331	0.0999
ERI	3.24	6.91	1033	0.0780
ITQ-29	3.66	10.58	1079	0.1216

both the characteristic pore sizes and the accessible space using helium (kinetic radius of 1.3 Å) as a probe molecule for the targeted zeolites. The channel-like topology of OFF means slight differences between the PLD and the LCD; LCD is about twice the value of the PLD in the cagelike zeolites and even more in the case of ITQ-29. The LCD of the latter is further larger than that of the remaining zeolites, which is approximately 7 Å. In addition, Figure 2 displays the pore size distributions to provide information on the void space that corresponds to certain pore sizes. Virtually the whole accessible space in CHA, ERI, and ITQ-29 corresponds to the cages.

Figure 3 shows the heats of adsorption and Henry coefficients as a function of chain length for alkanes and their respective 2- and 4- alkenes for the four considered all-silica zeolites at 600 K. Results are qualitatively in agreement because they are closely related magnitudes. Data for alkanes agree with those previously reported.[8−11] As occurs for alkanes, the heat of adsorption and Henry coefficients of alkenes in OFF increase linearly with carbon chain length because the enthalpy gained by molecule−wall interaction outweighs the loss in entropy. Only tiny differences in their respective values can be observed regardless of the position of the double bond. For the remaining zeolites, the window effect found for alkanes is also observed for the studied alkenes: ERI- and CHA-structures show a nonmonotonic, periodic behavior, which occurs also for ITQ-29 but only for chains longer than 21 carbon atoms. The local maxima in Henry coefficients indicate that the shape of chains with 5 or 6 carbon atoms is commensurate with that of a CHA-type cage, whereas in ERI-type cage it occurs for chains lengths of 8 or 9 atoms. These extrema are maintained for all the plotted hydrocarbons. The following sharp decrease denotes that the molecules are forced to curl up so as to fit into a single cage. When they are even longer, this conformation becomes too unfavorable and they stretch across two cages instead, as reflected in the local minima in both magnitudes. For alkanes, the first molecule to stretch across two cages is dodecane in CHA and tetradecane in ERI-type zeolite. These minima are slightly shifted toward larger chain lengths for the 2-alkenes in relation to the respective alkanes. When the double bond is located at a more intermediate position, in particular the fourth carbon, the window effect is found to be considerably less noticeable. Increasing the chain length improves adsorption again. Unlike the small, elongated CHA-

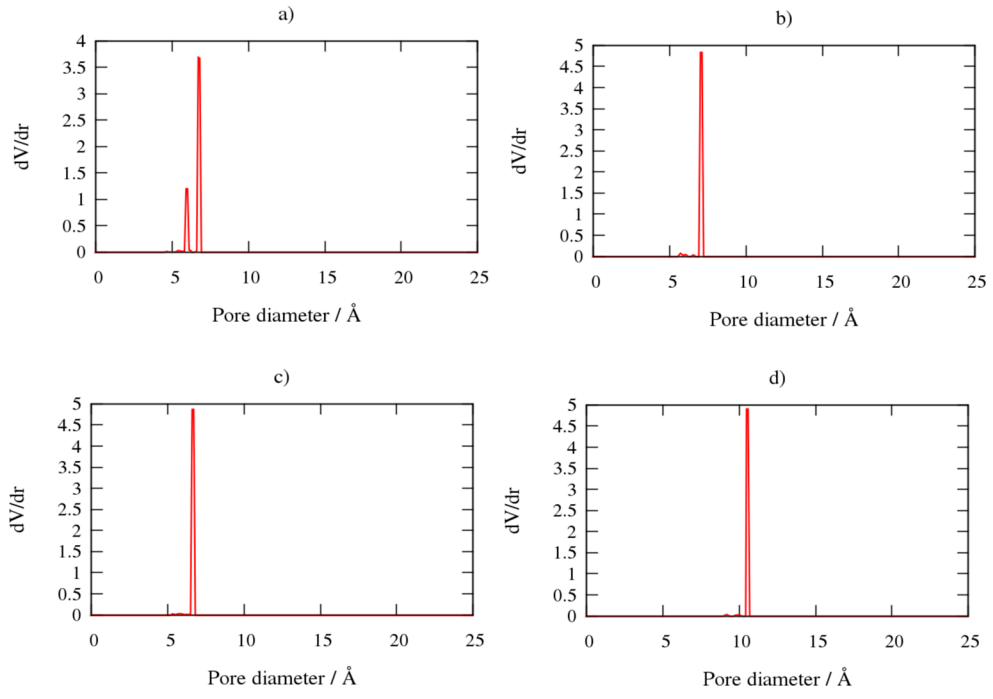

Figure 2. Pore size distributions of (a) OFF, (b) CHA, (c) ERI, and(d) ITQ-29 zeolites obtained using Zeo++ code[25] with a probe radius of 1.3 Å.

DOI: 10.1021/acs.jpcc.5b05597
J. Phys. Chem. C 2015, 119, 19236−19243

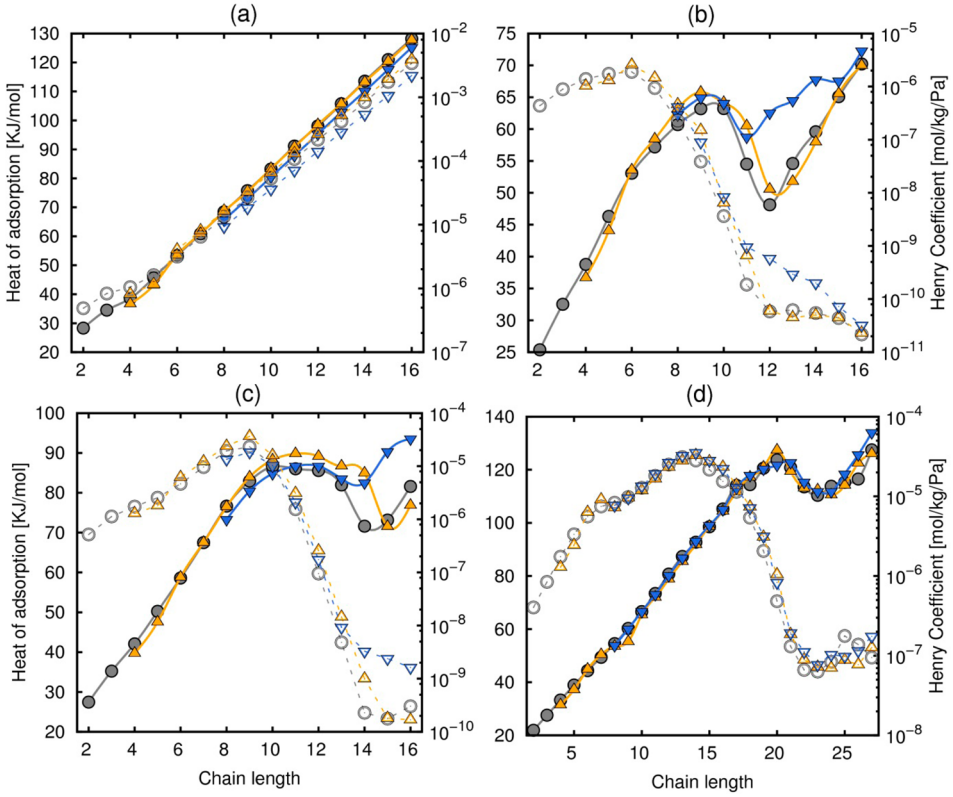

Figure 3. Henry coefficients (empty symbols) and heats of adsorption (solid symbols) as a function of the chain length of alkanes (gray symbols) and their respective alkenes with the double bond located in position 2 (yellow symbols) and position 4 (blue symbols) in (a) OFF, (b) CHA, (c) ERI, and (d) ITQ-29 zeolites at 600 K.

and ERI-type cages, molecules have more orientational freedom in the large, spherical LTA-type cages. The largest molecules that fit inside a single cage are these with 22−24 carbon atoms, and they represent the local minimum in the adsorption properties. In this case, results are virtually invariant with the presence and position of the double bond in the hydrocarbons. To illustrate the above information, Figure 4 displays snapshots from *NVT* calculations in all the zeolites for the specific case of 2-alkene with 20 carbon atoms. The figure allows one to neatly observe the stretching across two cages in CHA and ERI, whereas the adsorbate is still rolled up in the cage of ITQ-29.

To evaluate the influence of both the position and number of double bonds, we computed heats of adsorption in CHA and ERI zeolites for alkenes with two double bonds located in positions 1 and 4 (Figure 5). The respective minima reveal that the window effect of these unsaturated hydrocarbons becomes relatively less pronounced in CHA zeolite and virtually negligible in ERI. This can be explained in terms of the enthalpic and entropic variations. Tables S2−S7 of the Supporting Information provide the energies, enthalpies, and entropies of adsorption at zero coverage for all the systems. The increase (decrease in absolute value) of these magnitudes as consequence of the window effect diminishes for unsaturated hydrocarbons. As can be observed in Figure S1 of the Supporting Information, this phenomenon is however still present in ITQ-29 zeolite even for alkenes with a double bond every four carbon atoms. This can be attributed to the large size of the zeolite cages.

We find both the position and the number of double bonds of the guest hydrocarbons notably affect this quite unexplored cage phenomenon. To gain insight into the microscopic source,

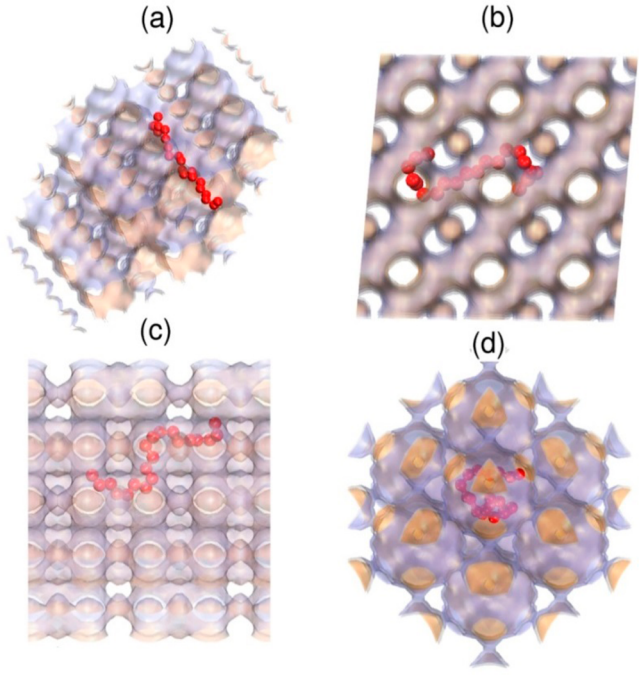

Figure 4. Snapshot of the molecular conformation of an unsaturated hydrocarbon of 20 carbon atoms and double bond in position 2 within the pores of (a) OFF, (b) CHA, (c) ERI, and (d) ITQ-29 zeolites at 600 K.

the molecular flexibility and conformation of the adsorbates is quantitatively evaluated. In Figure 6, we plot the average distance between the extreme carbon atoms of the hydrocarbon

DOI: 10.1021/acs.jpcc.5b05597
J. Phys. Chem. C 2015, 119, 19236−19243

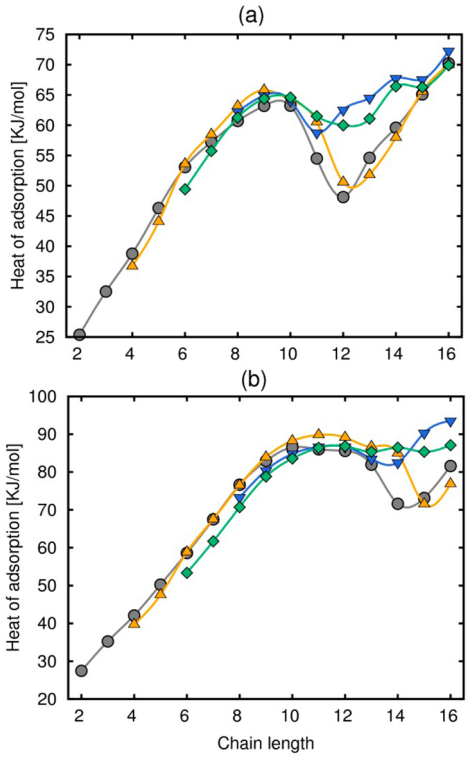

Figure 5. Heats of adsorption as a function of the chain length for alkanes (gray symbols) and their respective alkenes with the double bond located in position 2 (yellow symbols), position 4 (blue symbols), and both positions 1 and 4 (green symbols) in a) CHA and b) ERI zeolites at 600 K.

chain as a function of the chain length for saturated and unsaturated hydrocarbons in all the zeolites. The obtained curve is indeed in close relation with the adsorption behavior reported in the above figures. The position of the minima in heat of adsorption (or in Henry coefficients) indicates a crossover point. Below this crossover point, the molecules fit into a single cage; above this point, the chains start to find it energetically more favorable to stretch across two cages. This fact is clearly apparent from the plots in the cagelike structures, where abrupt increases of the average distance denoting the molecular stretching are observed at the previously commented chain lengths in each zeolite. In the channel-like OFF zeolite, we found the expected linear trend.

Figure 7 shows the distribution of the value along the time of the distance between the extreme carbon atoms of 2-alkenes for (i) a short chain (in blue), (ii) a chain commensurate with the framework cage (in yellow), and (iii) a longer chain (in violet) in the studied zeolites. The information obtained for alkanes and 4-alkenes is provided in Figures S2 and S3 of the Supporting Information, respectively. The fluctuating data with most probable values shifted from the average when the carbon chains are commensurate with the shape of the cages evidence the described unstable conformation. In addition, Figure S4 of the Supporting Information shows this distance as a function of the simulation time for the specific case of a 2-alkene with 20 carbon atoms in all the zeolites, providing quantitative data to the situations visualized in Figure 4. The lowest value, ca. 5 Å, corresponds to the ITQ-29 zeolite, denoting the rolling up of the hydrocarbon.

The different behavior of the saturated and unsaturated hydrocarbons when their chain lengths are commensurate with

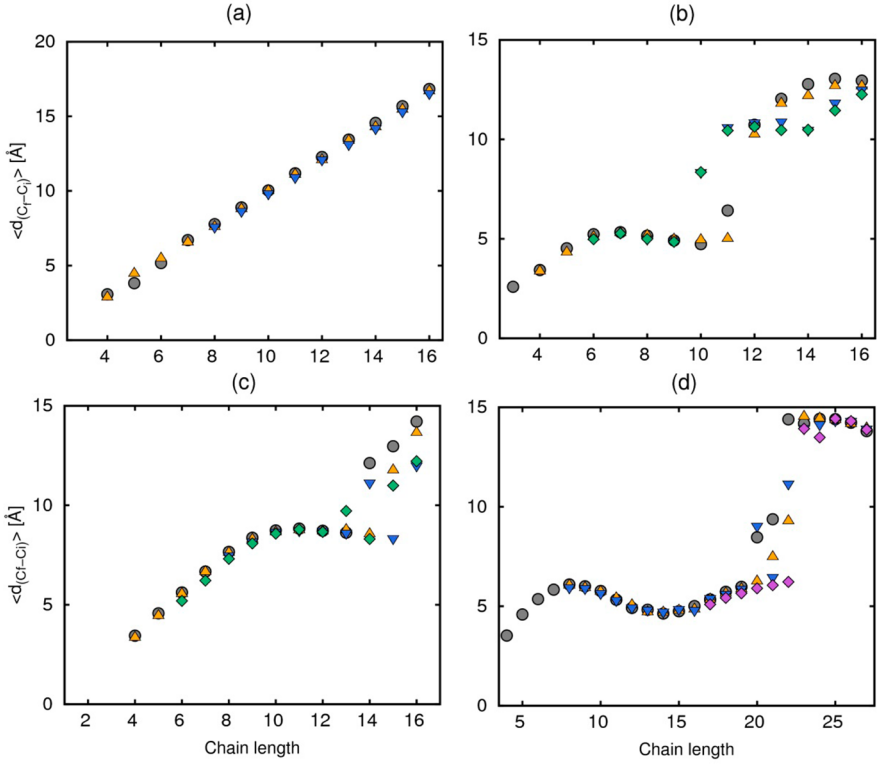

Figure 6. Average distance between the extreme carbon atoms of the hydrocarbons as a function of the chain length for alkanes (gray symbols) and their respective alkenes with the double bond located in position 2 (yellow symbols), position 4 (blue symbols), and both positions 1 and 4 (green symbols) in (a) OFF, (b) CHA, and (c) ERI zeolites, and also every four carbon atoms (pink symbols) in (d) ITQ-29 zeolite.

DOI: 10.1021/acs.jpcc.5b05597
J. Phys. Chem. C 2015, 119, 19236−19243

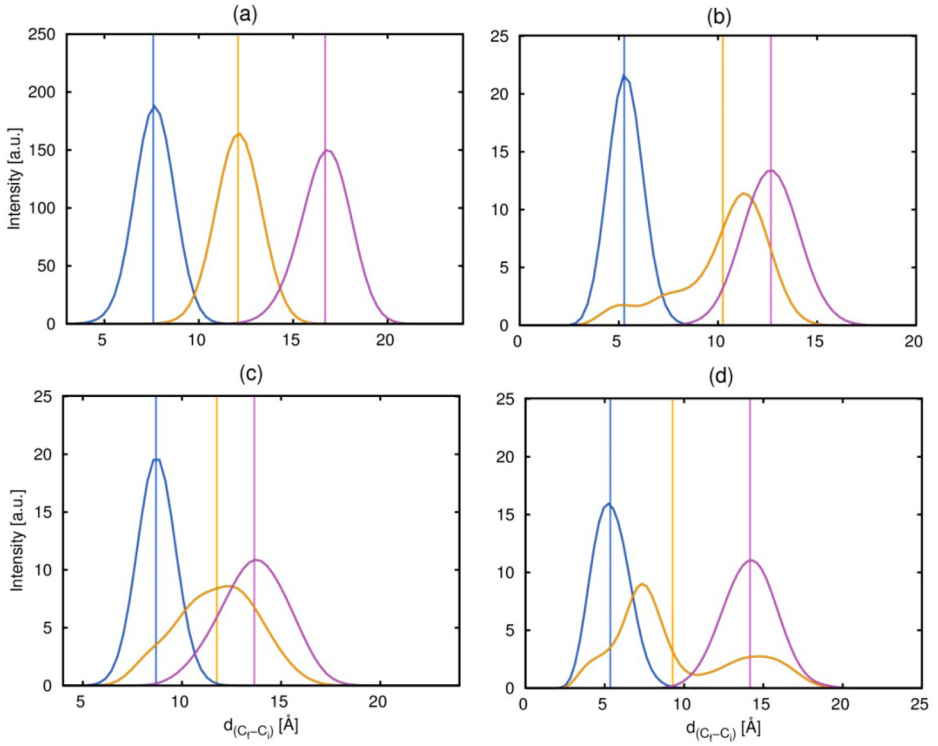

Figure 7. Distribution of the value along the time of the distance between the extreme carbon atoms of 2-alkenes with a short chain (blue), a chain commensurate with the zeolite cage (yellow), and a longer chain (violet) in (a) OFF, (b) CHA, (c) ERI, and (d) ITQ-29 zeolites.

the zeolite cages can be exploited for their separation. The efficiency of this type of selectivity (window effect) is next evaluated in terms of the Henry coefficients. This magnitude is a useful way to gauge if a material can be adsorption-selective. Particularly, the selectivity at low coverage for the separation of two molecules is estimated as the ratio of their Henry coefficients and allows one to qualitatively observe the separation ability of the structure in this regime. In Figure 8 (top panel), we plot the ratios of Henry constants for 4-alkene/alkane as a function of the chain length in CHA and ERI zeolites. Results for OFF and ITQ-29 zeolites are also displayed in Figure S5 of the Supporting Information. The selectivity is indeed remarkably larger for the chain lengths corresponding to window effects in each zeolite. Thus, CHA and ERI zeolites can be promising candidates for the separation of these hydrocarbons for chains of about 11−13 and 14−16 carbon atoms, respectively. As ERI exhibits the largest selectivity values, Figure 8 (bottom panel) shows the results for various hydrocarbon pairs in this specific zeolite. Those for CHA zeolite are given in Figure S6 of the Supporting Information. Specifically, we evaluated the separation of an alkane from the respective 2-alkene, 4-alkene, and *n*-1,4-diene, as well as of 4-alkenes from 2-alkenes. As can be seen, the selectivity for the separation of these adsorbate pairs increases notably for carbon chains of 14−16 atoms because of window effects, except for 2-alkene/alkane. Whereas ERI zeolite is the most selective for this binary mixture for chains shorter than 14 carbon atoms, this separation is notably less feasible for the range of chain lengths corresponding to cage effects in this zeolite. This is due to only slight variations in the behavior of the 2-alkene in relation to the alkane. As previously discussed, the relative weakness of the window effect is rather more significant for the 4-alkenes and *n*-1,4-dienes, which results in the displayed high values of selectivity. Results for 4-alkene/2-alkene reveal the effectiveness

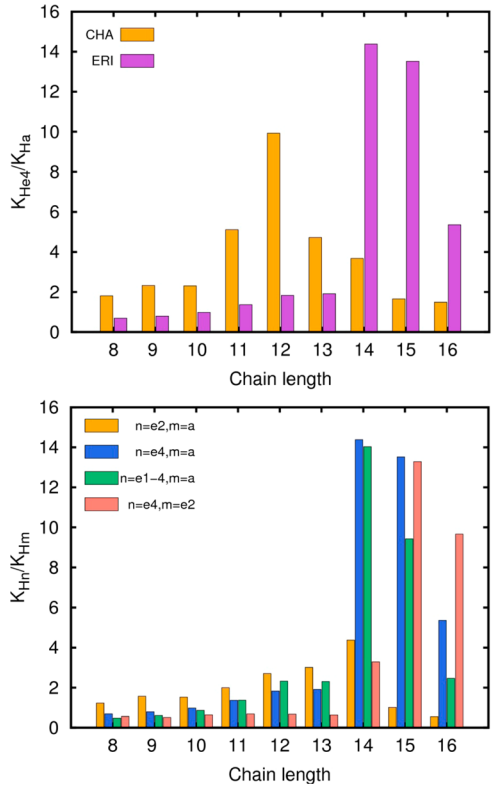

Figure 8. Selectivity at low coverage from Henry coefficients plotted against the chain length for 4-alkene/alkane separation in CHA and ERI zeolites (top) and for various adsorbate pairs in ERI zeolite (bottom) at 600 K. Nomenclature used for the hydrocarbons: alkane (a), alkenes with double bond in position 2 (e2), position 4 (e4), and positions 1 and 4 (e1−4).

DOI: 10.1021/acs.jpcc.5b05597
J. Phys. Chem. C 2015, 119, 19236−19243

of window effects for also separating unsaturated hydrocarbon isomers in regards to the position of the double bond.

The effect exerted on the heat of adsorption by the type of framework and by temperature is shown in Figure 9. Figure 9a

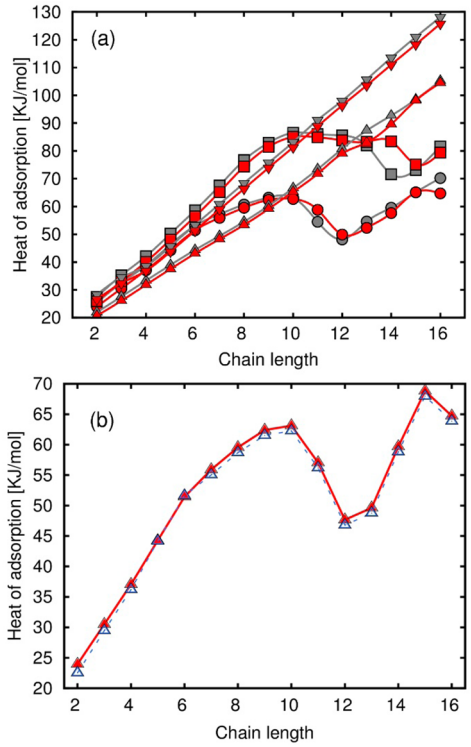

Figure 9. Isosteric heats of adsorption as a function of the hydrocarbon chain length for (a) alkanes (closed gray symbols) and 1-alkenes (closed red symbols) in OFF (down triangles), CHA (circles), ERI (squares), and ITQ-29 (up triangles) zeolites at 600 K and for (b) 1-alkenes at 600 K (red symbols) and 300 K (blue symbols) in CHA zeolite.

compiles the results of this property for alkanes and 1-alkenes in all the structures. For short chains, the heats of adsorption are quite similar in all structures except for ITQ-29, which exhibits lower values. This is consistent with the pore sizes reported in Table 1. For the hydrocarbons with the longest chains, the highest values of heats of adsorption were found for OFF, followed by ITQ-29, ERI, and CHA. In the 1D channel OFF, the hydrocarbons have strong interactions, and they curl up in ERI and CHA cavities, exhibiting the lowest interactions. Size and window effects lead to the different described situations at low-coverage regime for short and long chains. Finally, we have checked that temperature does not affect the window effect for the alkenes, as evidenced by Dubbeldam et al.[10] for alkanes. Figure 9b shows the isosteric heats of adsorption for 1-alkenes in CHA at 300 and 600 K. As expected, heat of adsorption is almost independent of temperature; therefore, the maximum for 10 carbon atoms and the minimum for 12 carbon atoms remain unaltered.

4. CONCLUSIONS

We performed molecular simulations of adsorption of hydrocarbons in zeolites to account for the influence exerted by the number and position of double bonds. When evaluating the heats of adsorption as a function of the chain lengths, we found alkenes to exhibit similar behavior to those previously reported for alkanes. In particular, they show a monotonic increasing trend for the channel-like OFF zeolite and window effects in the cagelike CHA, ERI, and ITQ-29 zeolites. The less conformational freedom induced by intermediate positions and mainly the presence of various double bonds in the alkenes lead to a weakness and even a vanishing of the window effect in CHA and ERI zeolites. Just slight deviations in enthalpy and entropy from the linearly increasing (in absolute value) tendency are appreciated for these alkenes with chain lengths commensurate with the cage sizes. Conversely, this is not the case in ITQ-29, where this phenomenon is preserved for the studied unsaturated hydrocarbons because of its notably larger cages. The different degrees of window effect for the targeted hydrocarbons were shown to be, in terms of the selectivity at low loading calculated from the Henry coefficients, efficient for olefin−paraffin and olefin−olefin separation applications. Although the largest computed values of selectivity correspond to ERI zeolite, the choice of the optimal cagelike zeolite exploiting this type of selectivity depends on the chain length. Because separations of light alkenes/alkanes are the most challenging and recognized to be a key technology in the petrochemical industry, structures with small cages would appear competitive in this respect.

■ ASSOCIATED CONTENT

Supporting Information

The Supporting Information is available free of charge on the ACS Publications website at DOI: 10.1021/acs.jpcc.5b05597.

Force field parameters; heats of adsorption as a function of the chain length for alkanes and a variety of alkenes in ITQ-29 zeolite; distribution of the distance value along the time between the extreme carbon atoms of alkanes and 4-alkenes in all the zeolites; distance between the extreme carbon atoms as a function of the simulation time for a 2-alkene of 20 carbon atoms in all the zeolites; values of selectivity at low-coverage for 4-alkenes/alkanes in all the zeolites and for various hydrocarbon pairs in CHA zeolite; and tables of energies, enthalpies, and entropies of adsorption computed at zero coverage for the systems at 600 K. (PDF)

■ AUTHOR INFORMATION

Corresponding Authors

*E-mail: pgomalv1@upo.es.
*E-mail: scalero@upo.es.

Notes

The authors declare no competing financial interest.

■ ACKNOWLEDGMENTS

This work is supported by the European Research Council through an ERC Starting Grant (ERC2011-StG-279520-RASPA), by the MINECO (CTQ2013-48396-P), and by the Andalucia Region (FQM-1851).

■ REFERENCES

(1) Weisz, P. B. Molecular Shape Selective Catalysis. *Pure Appl. Chem.* **1980**, *52*, 2091−2103.
(2) Csicsery, S. M. Catalysis by Shape Selective Zeolites - Science and Technology. *Pure Appl. Chem.* **1986**, *58*, 841−856.
(3) Gorring, R. Diffusion of Normal Paraffins in Zeolite T: Occurrence of Window Effect. *J. Catal.* **1973**, *31*, 13−26.

DOI: 10.1021/acs.jpcc.5b05597
J. Phys. Chem. C 2015, 119, 19236−19243

(4) Miale, J.; Chen, N. Y.; Weisz, P. Catalysis by Crystalline Aluminosilicates: Iv. Attainable Catalytic Cracking Rate Constants, and Superactivity. *J. Catal.* **1966**, *6*, 278−287.
(5) Chen, N.; Lucki, S.; Mower, E. Cage Effect on Product Distribution from Cracking over Crystalline Aluminosilicate Zeolites. *J. Catal.* **1969**, *13*, 329−332.
(6) Chen, N. Y.; Garwood, W. E. *Molecular Shape-Selective Hydrocarbon Conversion over Erionite*. In *Molecular Sieves*; American Chemical Society: Washington, DC, 1973; *121*, 575−582.
(7) Young, L. B. *Alkylation in Presence of Phosphorus-Modified Crystalline Luminosilicate Catalyst*. U.S. Patent 3,962,364, June 8, 1976.
(8) Dubbeldam, D.; Calero, S.; Maesen, T. L. M.; Smit, B. Understanding the Window Effect in Zeolite Catalysis. *Angew. Chem., Int. Ed.* **2003**, *42*, 3624−3626.
(9) Dubbeldam, D.; Calero, S.; Maesen, T. L. M.; Smit, B. Incommensurate Diffusion in Confined Systems. *Phys. Rev. Lett.* **2003**, *90*, 245901.
(10) Dubbeldam, D.; Smit, B. Computer Simulation of Incommensurate Diffusion in Zeolites: Understanding Window Effects. *J. Phys. Chem. B* **2003**, *107*, 12138−12152.
(11) Maesen, T. L. M.; Beerdsen, E.; Calero, S.; Dubbeldam, D.; Smit, B. Understanding Cage Effects in the N-Alkane Conversion on Zeolites. *J. Catal.* **2006**, *237*, 278−290.
(12) Calero, S.; Dubbeldam, D.; Krishna, R.; Smit, B.; Vlugt, T. J. H.; Denayer, J. F. M.; Martens, J. A.; Maesen, T. L. M. Understanding the Role of Sodium During Adsorption: A Force Field for Alkanes in Sodium-Exchanged Faujasites. *J. Am. Chem. Soc.* **2004**, *126*, 11377−11386.
(13) Dubbeldam, D.; Calero, S.; Vlugt, T. J. H.; Krishna, R.; Maesen, T. L. M.; Beerdsen, E.; Smit, B. Force Field Parametrization through Fitting on Inflection Points in Isotherms. *Phys. Rev. Lett.* **2004**, *93*, 088302.
(14) Dubbeldam, D.; Calero, S.; Vlugt, T. J. H.; Krishna, R.; Maesen, T. L. M.; Smit, B. United Atom Force Field for Alkanes in Nanoporous Materials. *J. Phys. Chem. B* **2004**, *108*, 12301−12313.
(15) Daems, I.; Baron, G. V.; Punnathanam, S.; Snurr, R. Q.; Denayer, J. F. M. Molecular Cage Nestling in the Liquid-Phase Adsorption of N-Alkanes in 5a Zeolite. *J. Phys. Chem. C* **2007**, *111*, 2191−2197.
(16) Suib, S. L. Handbook of Zeolite Science and Technology. *Science* **2003**, *302*, 1335−1336.
(17) Liu, B.; Smit, B.; Rey, F.; Valencia, S.; Calero, S. A New United Atom Force Field for Adsorption of Alkenes in Zeolites. *J. Phys. Chem. C* **2008**, *112*, 2492−2498.
(18) Frenkel, D.; Smit, B. *Understanding Molecular Simulation: From Algorithms to Applications*; Academic Press: San Diego, CA, 2001.
(19) Ortiz-Roldan, J. M.; Vicent-Luna, J. M.; Ruiz-Salvador, A. R.; Calero, S.; Hamad, S. Personal comunication.
(20) Dubbeldam, D.; Torres-Knoop, A.; Walton, K. S. On the Inner Workings of Monte Carlo Codes. *Mol. Simul.* **2013**, *39*, 1253−1292.
(21) Dubbeldam, D.; Calero, S.; Ellis, D. E.; Snurr, R. Q. Raspa: Molecular Simulation Software for Adsorption and Diffusion in Flexible Nanoporous Materials. *Mol. Simul.* **2015**, 1−21.
(22) Widom, B. Some Topics in the Theory of Fluids. *J. Chem. Phys.* **1963**, *39*, 2808−2812.
(23) Nose, S. A Molecular Dynamics Method for Simulations in the Canonical Ensemble. *Mol. Phys.* **2002**, *100*, 191−198.
(24) Hoover, W. G. Canonical Dynamics - Equilibrium Phase-Space Distributions. *Phys. Rev. A: At., Mol., Opt. Phys.* **1985**, *31*, 1695−1697.
(25) Willems, T. F.; Rycroft, C.; Kazi, M.; Meza, J. C.; Haranczyk, M. Algorithms and Tools for High-Throughput Geometry-Based Analysis of Crystalline Porous Materials. *Microporous Mesoporous Mater.* **2012**, *149*, 134−141.
(26) Foster, M. D.; Rivin, I.; Treacy, M. M. J.; Friedrichs, O. D. A Geometric Solution to the Largest-Free-Sphere Problem in Zeolite Frameworks. *Microporous Mesoporous Mater.* **2006**, *90*, 32−38.
(27) Lee, B.; Richards, F. M. The Interpretation of Protein Structures: Estimation of Static Accessibility. *J. Mol. Biol.* **1971**, *55*, 379−400.

DOI: 10.1021/acs.jpcc.5b05597
J. Phys. Chem. C 2015, 119, 19236−19243